

Final Draft
of the original manuscript:

Angelova, A.; Drechsler, M.; Garamus, V.; Angelov, B.:

Pep-Lipid Cubosomes and Vesicles Compartmentalized by Micelles from Self-Assembly of Multiple Neuroprotective Building Blocks Including a Large Peptide Hormone PACAP-DHA.

In: ChemNanoMat : chemistry of nanomaterials for energy, biology and more.
Vol. 5 (2019) 11, 1381 - 1389.

First published online by Wiley: September 17, 2019

DOI: 10.1002/cnma.201900468

<https://doi.org/10.1002/cnma.201900468>

Pep-Lipid Cubosomes and Vesicles Compartmentalized by Micelles from Self-Assembly of Multiple Neuroprotective Building Blocks Including a Large Peptide Hormone PACAP-DHA

Angelina Angelova^{1,*}, Markus Drechsler², Vasil M. Garamus³, Borislav Angelov^{4,*}

¹Institut Galien Paris-Sud, CNRS UMR 8612, Univ. Paris-Sud, Université Paris-Saclay, LabEx LERMIT, F-92290 Châtenay-Malabry cedex, France,

²Keylab "Electron and Optical Microscopy", Bavarian Polymerinstitute (BPI), University of Bayreuth, D-95440 Bayreuth, Germany,

³Helmholtz-Zentrum Geesthacht: Centre for Materials and Coastal Research, D-21502 Geesthacht, Germany,

⁴Institute of Physics, ELI Beamlines, Academy of Sciences of the Czech Republic, Na Slovance 2, CZ-18221 Prague, Czech Republic.

*E-mails: Angelina.Angelova@u-psud.fr; Borislav.Angelov@eli-beams.eu

KEYWORDS: Cryo-TEM, BioSAXS; pituitary adenylate cyclase-activating polypeptide (PACAP38); peptide amphiphile; liquid crystalline nanoassemblies; lipid cubic phase; cubosomes; docosahexaenoic acid (DHA)

ABSTRACT

Structural control over membrane shape transformations is important for understanding of living nanoscale topologies as well as for the design of nanomedicines by self-assembly. Disease-modifying drug delivery strategies can slow down the progress of neurological disorders thanks to macromolecular therapeutics, which are highly selective. Because of their low bioavailability, supramolecular nanoprodrugs and interface-rich liquid crystalline nanocarriers can be used for more efficient delivery of peptide ligands (including high molecular weight peptide hormones) to their target sites. Here an amphiphilic construct of the pituitary adenylate cyclase-activating polypeptide (PACAP38) coupled to an ω -3 polyunsaturated fatty acid (docosahexaenoic acid (DHA)) is designed. The hormone PACAP38 is a ligand of the class B PAC1 G-protein-coupled receptor (GPCR), whereas the lipid trophic factor DHA is a ligand of the retinoid X receptor (among other biological functions). We report on the spontaneous assembly of the synthetic lipopeptide building blocks PACAP-DHA in (i) PEGylated antioxidant-containing micelles and (ii) lipid cubic membranes as nanochannel network reservoirs (pep-lipid cubosomes). The structural organization of the created nano-assemblies and nanoparticles is determined by synchrotron small-angle X-ray scattering (BioSAXS) and cryogenic transmission electron microscopy (cryo-TEM) at high resolution. The results revealed that the peptide amphiphile PACAP-DHA is assembled in original multicompartiment liquid crystalline membrane-based architectures. Their topologies involve intriguing ladybird-like biomimetic patterns and interface-rich nanostructures, which are promising for sustained-release applications in neuro-regenerative strategies.

Introduction

Current concepts of molecularly engineered biomimetic assemblies appear to be fruitful for the design of internally nanostructured materials, nanoparticles of mesoporous topologies, nanosheets, nanotubules, interface-rich biocompatible scaffolds, and hierarchical type constructs.¹⁻¹⁶ The progress in nanomedicine and regenerative therapies incessantly requires smart nanocarriers for drug delivery and novel supramolecular nanoprodrugs of improved efficacy.¹⁷⁻²⁶ Self-assembly of prodrugs into nanoparticles can ensure high drug content and carrier-free drug delivery.²⁷⁻³³ The attachment of lipophilic moieties to hydrophilic drug molecules enhances the bioavailability of the therapeutic agents.^{27, 30} Thus, efficient delivery can be achieved using prodrug nanoassemblies with elevated concentrations of the therapeutic substances.^{27, 30}

Neurological diseases (Alzheimer's (AD) and Parkinson's (PD) diseases, and amyotrophic lateral sclerosis (ALS)) are multi-factor disorders and therefore require targeting of multiple signaling pathways towards regeneration.³⁴⁻³⁸ Targeted therapies of neurodegenerative disorders demand safe disease-modifying drug delivery systems.^{18, 23, 36-42} Despite of the big investments, symptom-modifying medicines have failed to treat the inherent disease causes.³⁴ This emphasizes the necessity of alternative therapeutic concepts and delivery approaches.^{34, 36} We consider that multifunctional self-assembled cubosome nanoparticles with internal compartments for enhanced upload of neuroprotective molecules may be excellent candidates for innovation in neuro-regenerative therapies. We investigate the supramolecular co-assembly of several therapeutic building blocks into hierarchically-organized biocompatible nanostructures. In this

approach, particular advantages are associated with the inner organization of the interface-rich nanoarchitectures of multi-material compositions.

Our purpose is to create interface-rich pep-lipid nanostructures with multifunctional molecular building blocks. Figure 1 presents the functionalities and the chemical structures of the compounds serving as building blocks of pep-lipid-based self-assembled nanomedicines of high drug content. Among the considered lipophilic moieties, docosahexaenoic acid (DHA) (C22:6) is chosen as a natural long chain ω -3 polyunsaturated fatty acid (PUFA), which is especially beneficial for human health.^{43–53} DHA is an important factor in many cellular functions (see *SI* for details about the DHA role). The bioactive building block DHA plays a crucial role in the control of the phospholipid membrane organization.^{54–67} Our recent super-resolution STED microscopy investigation has revealed the effect of docosahexaenoic acid on the nanoscale clustering and oligomerization of the neurotrophin membrane receptor TrkB, which is responsible for the neuronal cell survival and the maintenance of the neuronal functions.⁶⁶

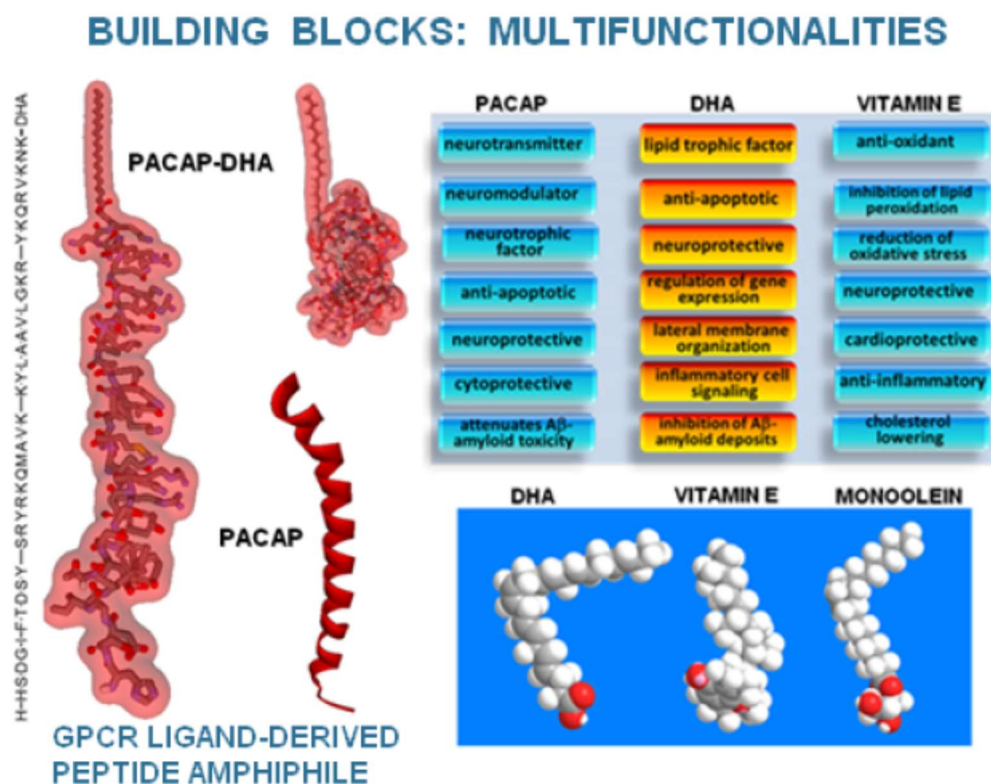


Figure 1. Strategy for co-assembly of molecular building blocks with multiple functionalities into nanocarriers of high drug content. Molecular structure of the GPCR ligand-derived peptide amphiphile PACAP-DHA. The synthetic construct consist of two bioactive components: the pituitary adenylate cyclase-activating polypeptide (PACAP38) and the long-chain ω -3 polyunsaturated fatty acid DHA (C22:6). The peptide amphiphile PACAP-DHA is presented in an extended state (left) and in a folded configuration (right) with regard to the non-modified peptide PACAP38 (bottom panel). The biological functions of the building blocks PACAP (pituitary adenylate cyclase-activating polypeptide), DHA (docosahexaenoic acid), and vitamin E α -tocopherol (vitamin E) are schematically indicated.

In the present design, the lipid trophic factor DHA is bound to the neuropeptide PACAP (pituitary adenylate cyclase-activating polypeptide) [a second therapeutic building block] in order to create a bioactive amphiphile with dual functions. Both DHA and PACAP may cross the blood-brain barrier (BBB) to exert their effects. However, they are especially deficient under

pathological and stress conditions.⁶⁷ As a consequence, these therapeutic compounds need to be delivered by suitable safe carriers to the central nervous system (CNS) or to particular tissues. PACAP is a high-molecular-weight neuropeptide ligand of the PAC1 membrane receptor (a class B GPCR), which is widely distributed in the brain and other organs.⁶⁸⁻⁷⁸ As a 38-amino acid peptide (Fig. 1, bottom panel), PACAP stimulates the cAMP formation in pituitary cells through its hormone activity.^{69,70} It exhibits strong anti-apoptotic effects in neuronal and non-neuronal cells.⁷²⁻⁷⁸ PACAP has been reported to increase the levels of the anti-apoptotic proteins p-Akt, p-ERK1, p-ERK2, PKC, and Bcl-2. This leads to diminished levels of activated caspases and in a decreased phosphorylation of the pro-apoptotic protein p38MAPK.⁷¹ Therefore, this peptide appears to be a neurotrophic factor.^{72,78} It is protective in retinal pathologies and contributes to retinal regeneration by attenuating the apoptosis of the retinal neurons (see *SI* for more details about the biological role of PACAP).

The purpose of the present work is to determine the structural organization of the soft multicomponent nanoarchitectures into which the novel synthetic high-molecular-weight PACAP-DHA double-ligand peptide amphiphile (Fig. 1) is assembled with the help of neutral and bioactive lipids. The stability of the nanoassemblies formed by the lipophilic ingredients (DHA, vitamin E and monoolein (MO)) is achieved by inclusion of the PEGylated surfactant vitamin E α -tocopheryl polyethylene glycol 1000 succinate (VPGS-PEG1000). Small amounts of this nonionic amphiphile may provide steric stabilization of the obtained nanocarrier dispersions.⁷⁹ The antioxidant vitamin E α -tocopherol (Fig. 1) is chosen as a lipophilic additive for its ability to prevent the lipid oxidation. Vitamin E is a potential therapeutic compound in neuro-regeneration, suppression of oxidative stress and reduction of the A β -amyloid peptide plaque in AD.^{37,39,40} We employed DHA both as a pure lipid and in its bound state to the PACAP ligand.

High resolution structural methods, namely synchrotron small-angle X-ray scattering (SAXS) and cryogenic transmission electron (cryo-TEM) microscopy, are employed to study the self-assembled nanostructures embedding the PACAP-DHA peptide amphiphile. This structural knowledge is required for control of the envisioned sustained-release properties of the resulting scaffolds. The structural features of the generated multicompartment nanoassemblies are considered with regard to the topologies of other biomimetic and bioinspired sophisticated nanoscale architectures.⁷⁹⁻⁹⁴

Scattering patterns of carrier-free PACAP-DHA and PACAP peptides in solutions.

The PACAP-DHA peptide amphiphile was custom synthesized by coupling of the ω -3 polyunsaturated lipid docosahexaenoic acid (DHA) to the free Lys-38 residue of the C-terminal of the PACAP38 polypeptide. The attempts to obtain nanodispersions of PACAP-DHA by the method of nanoprecipitation of prodrugs³¹ failed owing to the hydrophobic/hydrophilic balance of the macromolecule (Fig. 1). It turned out to be much less hydrophobic as compared to the common lipid-based prodrugs,²⁷ which lack a peptide building block. In the next step, we studied the self-assembly properties of the new biomacromolecule PACAP-DHA in a carrier-free state in solutions and upon inclusion in liquid crystalline nanocarriers. Figure 2A shows the SAXS pattern of the DHA-modified pituitary adenylate cyclase-activating polypeptide (PACAP-DHA) with regard to that of the native polypeptide PACAP (presented in Fig. 1). The difference in the recorded solution scattering curves reveals a structural change in the supramolecular organization of the polypeptide owing to the covalent coupling of the long chain ω -3 PUFA. The distance distribution $p(r)$ function derived from the SAXS pattern evidenced that the peptide amphiphile PACAP-DHA self-assembles into supramolecular aggregates in aqueous environment. For the investigated PACAP-DHA concentration (6 mM), the estimated gyration radius, R_g , of 67.7 nm corresponds to a notable clustering of the biomacromolecules in the aqueous medium. The slope of the SAXS curve at low q -values and its overall shape revealed a coexistence of prolate and spherical nanoparticles in the dispersion. An experimental gyration radius value, R_g , of 13.0 nm was determined by SAXS for the native peptide PACAP38 in a concentrated solution (10 mg/mL) state (Fig. 2A). A gyration radius value R_g of 2.2 nm was obtained for PACAP in a monomeric state upon dilution. The propensity of the concentrated peptides for clustering and aggregation may be explained by the hydrophobic interactions between the lipid moieties of the PACAP-DHA macromolecules and/or by the association of the hydrophobic N-terminal regions of the polypeptide chains. Despite of the self-assembly propensity, the obtained supramolecular PACAP-DHA assemblies were not stable enough at room temperature in a solution phase on a long term due to the DHA oxidation. For this reason, we proceeded toward incorporation of the peptide amphiphile in stably-existing protective nanocarriers.

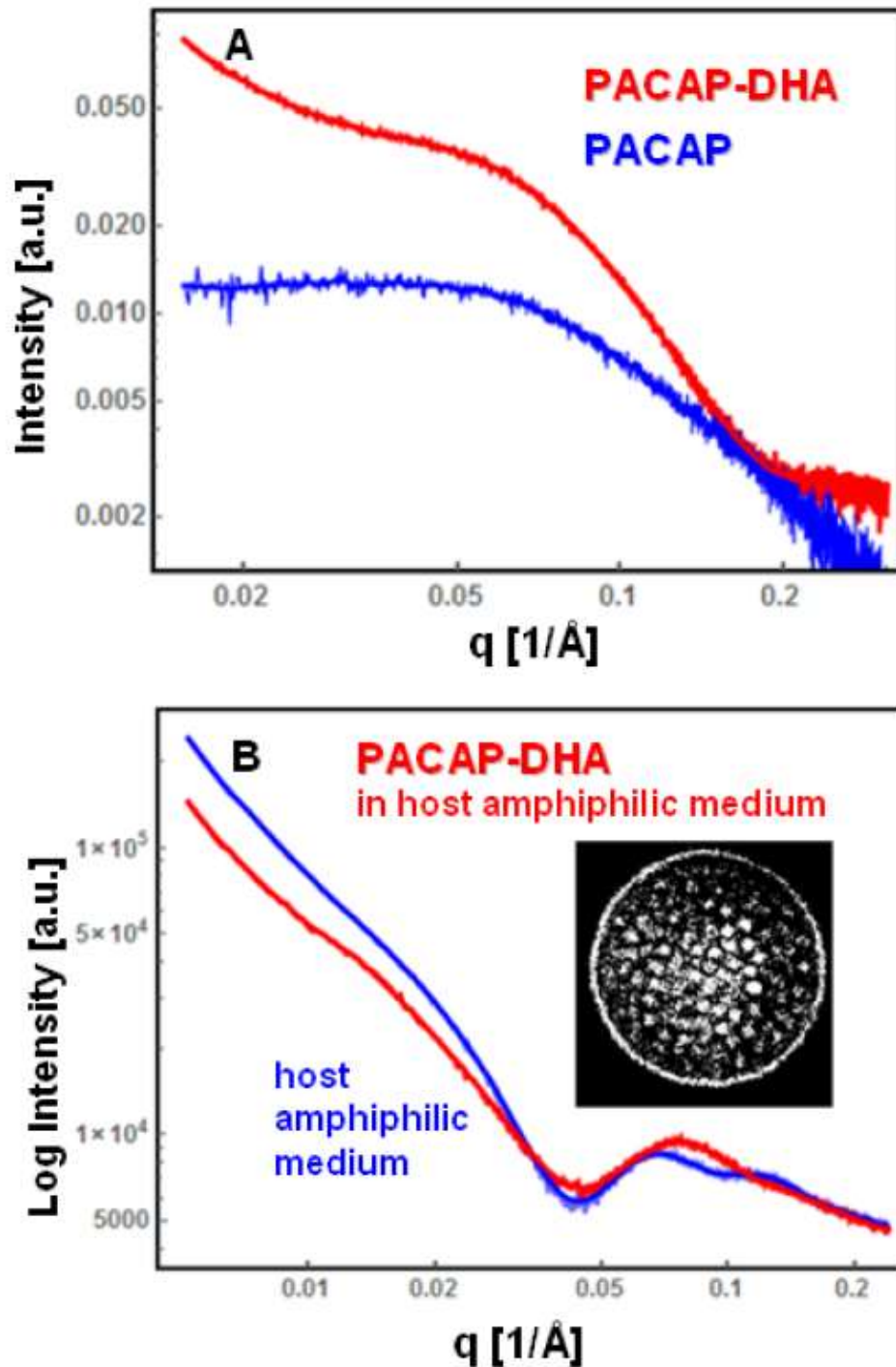


Figure 2. Synchrotron small-angle X-ray scattering (SAXS) patterns of the PACAP-DHA peptide construct in an aqueous solution (A) and in PEGylated amphiphilic assemblies (B). (A) SAXS patterns of PACAP-DHA (red plot, PACAP bound to a docosahexaenoic acid; 6 mM concentration) and of a native PACAP polypeptide (blue plot; 10 mg/mL concentration). (B) SAXS patterns characterizing the self-assembled PACAP-DHA/vitamin E/VPGS-PEG1000 amphiphilic mixture (red plot) and an equivalently concentrated DHA/vitamin E/VPGS-PEG1000 system without a bound peptide PACAP. The blue plot corresponds to mixed DHA/vitamin E/VPGS-PEG1000 assemblies (54/23/23 molar ratio) obtained upon functionalization of the PEGylated VPGS-PEG1000 micelles by the lipid trophic factor DHA and the antioxidant vitamin E α -tocopherol. Temperature: 20 °C. Inset: Topology of the self-assembled core-shell structures deduced from a processed cryo-TEM image.

Supramolecular assembly of PACAP-DHA with an antioxidant-containing host amphiphile medium

The PACAP-DHA peptide amphiphile was embedded in a membrane-like medium containing a protective antioxidant (vitamin E α -tocopherol) and a PEGylated agent (VPGSPEG1000). Bearing in mind the large molecular mass of the PACAP polypeptide (4.5 kDa) and its length in an extended state conformation (5.4 nm) (Fig. 1), two lipophilic building blocks, DHA and vitamin E (Fig. 1), were included in the amphiphilic carriers of vitamin E α -tocopheryl polyethylene glycol 1000 succinate (VPGS-PEG1000) in order to create a membrane mimetic medium with an increased volume of the hydrophobic domain. The aim was to counterbalance the diminishment of the mean critical packing parameter²⁰ of the pep-lipid-surfactant system due to the presence of a large aminoacid-sequence moiety. It is worth to note that the synthetic PACAP-DHA molecule has a net charge of +8 at pH 7, which augments its hydrosolubility with regard to a typical lipid-based prodrug.³⁰ The PEGylated corona (VPGS-PEG1000) was placed in order to enhance the stability of the generated nanoparticles in a dispersed state. The proposed multi-level self-assembly approach is motivated also by the fact that sterically-stabilized micelles involving polyethylene glycol (PEG) chains may amplify the bioactive properties of solubilized peptides.⁷⁷ So far, NMR studies have demonstrated that the unmodified PACAP polypeptide is soluble in dodecylphosphocholine phospholipid micelles.⁷⁷ Precise control over the structural organization of the studied PACAP-DHA/vitamin E/VPGS-PEG1000 amphiphilic systems was achieved by synchrotron SAXS measurements (Fig. 2B, red plot) and cryo-TEM imaging (Fig. 3). The SAXS pattern of the DHA/vitamin E/VPGSPEG1000 self-assembled mixture is shown for a comparison (Fig. 2B, blue plot). The obtained SAXS results indicated that the host VPGS-PEG1000 micellar solution is transformed into a dispersion of supramolecular amphiphilic aggregates of mixed compositions, which comprise a bimodal distribution of particle sizes. The created new nanoparticles are bigger in size (diameters above 100 nm) as compared to the initially formed monodispersed PEGylated micelles of a mean diameter $d=11$ nm. We note that the resulting SAXS curves (Fig. 2B) considerably differ from that of the carrier-free PACAP-DHA peptide amphiphile (Fig. 2A) and also from that of the surfactant micelles (Fig. S1). This reveals the structural transition triggered by the pep-lipid functionalization. The formation of stable PEGylated amphiphilic dispersions evidenced the preference of PACAP-DHA for encapsulation in a membrane mimetic environment. In the following, the obtained supramolecular structures are directly visualized by cryo-TEM imaging.

Topological features of PEGylated pep-lipid supramolecular aggregates

The propensity of the peptide amphiphile PACAP-DHA for spontaneous assembly with protective antioxidant-containing nanocarriers (vitamin E/VPGS-PEG1000) was established by cryo-TEM imaging (Fig. 3) as well. The morphological features of the mixed PACAPDHA/vitamin E/VPGS-PEG1000 dispersions confirmed the induction of new multicompartement supramolecular structures and the coexistence of small and large PEGylated nanoassemblies. The lipid DHA/vitamin E/VPGS-PEG1000 nanocarriers formed vesicle-like shells at a DHA content equivalent to that in the PACAP-DHA-containing amphiphilic mixtures. These structures likely result from the bilayer membrane-type packing of the DHA and vitamin E components. Evidently, the single chain DHA lipid associates with vitamin E in the shape of a double-chain amphiphile, which forms bilayer vesicles. Coexisting small spherical and elongated nanoparticles were found to be encapsulated in bigger closed-bilayer shells. Such structures were observed by cryo-TEM imaging before and after the inclusion of PACAP polypeptide chains as building blocks of the supramolecular assemblies.

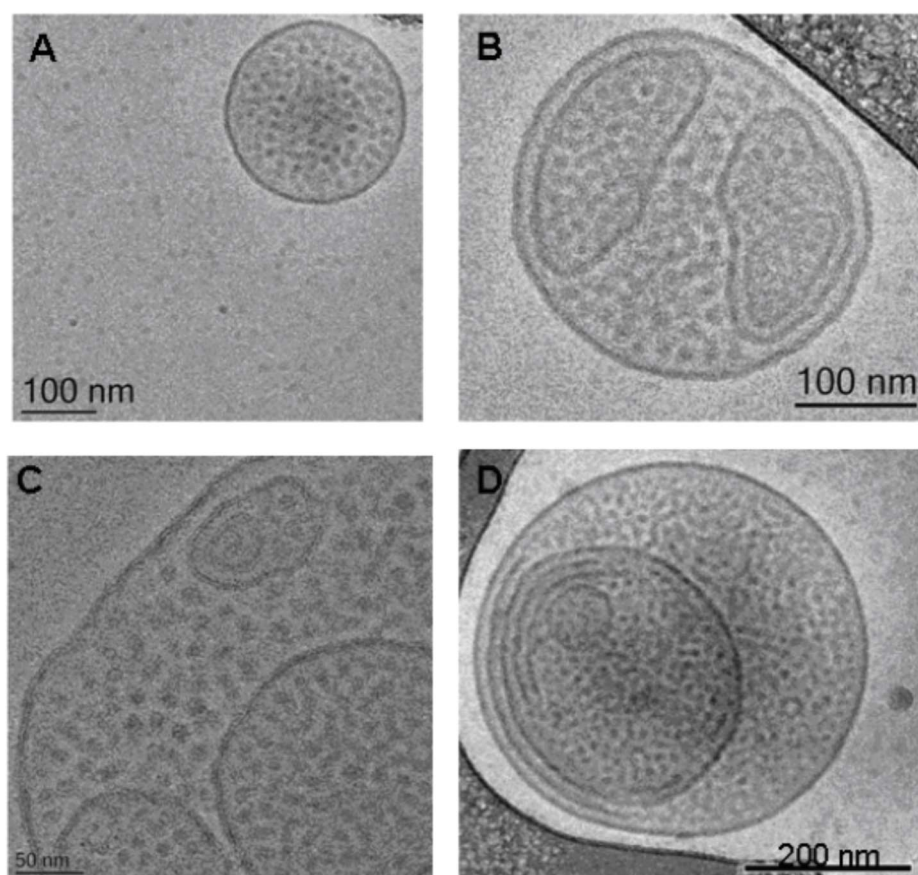


Figure 3. Cryo-TEM microscopy images of pep-lipid carriers with hierarchical organizations and internal compartments. (A) Membrane-mimetic environment of DHA/vitamin E/VPGSPage PEG1000 assemblies into which the peptide PACAP is embedded at a concentration 4 mg/mL (B). (C, D) Images of PACAP-DHA/vitamin E/VPGS-PEG1000 assemblies obtained at an equivalent molar ratio of the lipid components (DHA/vitamin E/VPGS-PEG1000, 54/23/23 molar ratio). The revealed hierarchical organization comprises a coexistence of small micelles and micellovesicular containers. The generated vesicular membranes evolve to close shells that encapsulate smaller lpep-lipid aggregates (D). Their projections are viewed as ladybird-like (Coccinelle) patterns (B,C).

The topological transformation of the host PEGylated micelles (VPGS-PEG1000) into hybridtype pep-lipid nanoparticles was examined in more detail in relation to the incorporation of the peptide amphiphile PACAP-DHA in the host membrane-mimetic medium. The small micellar aggregates were found to occupy variable fractions of the projected planes in the cryo-TEM images as they get modified by the PACAP polypeptide chain (Fig. 3B,C). The high resolution micrographs revealed the development of compartmentalized supramolecular architectures characterized by intriguing ladybird-like (Coccinelle) patterns (Fig. 3B,C). They imply the formation of micello-vesicular containers starting from lipid bilayer membrane fragments and shells. The vesicular reservoirs have mean diameters in the range from 150 nm to 350 nm. The observed hybrid morphologies (Fig. 3) corroborate with the occurrence of a structural transition, which was evidenced by the SAXS analysis (Fig. 2).

A closer inspection of the images in Fig. 3 by the *Image J* software (National Institutes of Health) established that the spatial arrangement in the compartmentalized amphiphilic aggregates represents a network packing of small objects inside the vesicular reservoirs of mixed amphiphilic compositions (see the inset in Fig. 2B). The achievement of the hybrid micellovesicular organization appears to be preceded by curvature changes and fusion of the spherical micelles into more extended structures. This favours the development of flexible amphiphile/water interfaces, which may transform the vesicular membranes into closed containers (Fig. 3D).

The obtained cryo-EM images reflected the electron density contrast resulting from the lipid headgroup/water interfaces in the mixed DHA/vitamin E/VPGS-PEG1000 assemblies. The polypeptide chains of the PACAP-DHA amphiphile are challenging to be straightforward visualized owing to their low electron density. Nevertheless, the core structures of the vesicular

containers, observed as a matrix of dots in the cryoTEM images, should enclose PACAP polypeptide chains which are bound to the DHA building blocks. Owing to the insufficient electron density contrast, the polymeric PEG chains of VPGS-PEG1000 cannot be visualized as a Stealth shell at the nanoparticles peripheries as well.

Cubic-phase liquid crystalline nanocarriers (cubosomes) embedding PACAP-DHA

The peptide amphiphile PACAP-DHA is expected to show affinity for incorporation in lipid membranous assemblies, which may stabilize the peptide conformation as in native membranous systems.⁶⁹ We exploited the fact that PEGylated cubosome containers with distinct internal hydrophobic and hydrophilic compartments are highly efficient for peptide nanodrug formulation.^{4, 6, 41} Here a nanostructured liquid crystalline membrane medium was created using cubic-phase assemblies of the hydrated nonlamellar lipid monoolein (MO). Appropriate amounts of the lipid trophic factor DHA and the antioxidant vitamin E (α -tocopherol) were included towards functionalization of the cubic phase matrix. The stability of the dispersed lipid assemblies was achieved through PEGylation, which was realized upon inclusion of the VPGS-PEG1000 amphiphile. The obtained structural results refer to MO/DHA/vitamin E/VPGS-PEG1000 nanoassemblies of a lipid molar ratio 69/18/9/4, at which the peptide amphiphile PACAP-DHA was incorporated in the assembly.

Figure 4A presents the SAXS patterns of highly hydrated cubosome particles PACAPDHA/MO/DHA/vitamin E/VPGS-PEG1000, which were dispersed in an excess aqueous phase. The liquid crystalline inner cubic lattice periodicities were evident before and after the incorporation of the positively-charged PACAP-DHA construct.

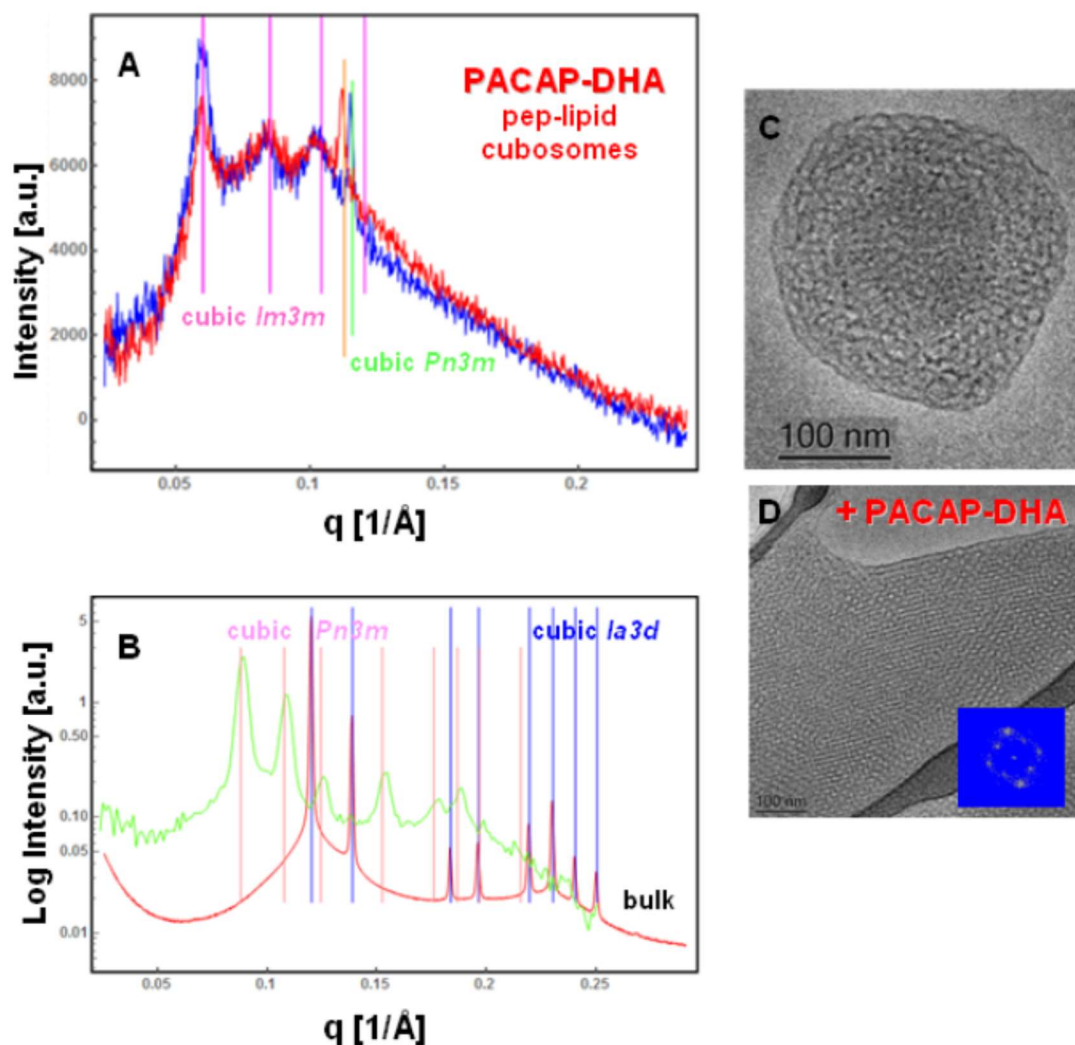


Figure 4. Synchrotron SAXS patterns of pep-lipid cubosomes. (A) Nanodispersions obtained at full hydration. The peptide amphiphile PACAP-DHA is embedded in liquid crystalline nanochanneled network reservoirs formed by the MO/DHA/vitamin E/VPGS-PEG1000 cubic phase mixture (lipid molar ratio 69/18/9/4) in excess aqueous medium. The red plot corresponds to the amphiphilic composition PACAP-DHA/MO/DHA/vitamin E/VPGS-PEG1000, whereas the blue plot refers to the MO/DHA/vitamin E/VPGS-PEG1000 assemblies. The molar fraction of the

PACAP-DHA peptide amphiphile is 1/50 with regard to the DHA lipid. The detected Bragg peaks provide evidence for periodic cubic lattice organizations and the formation of pep-lipid cubosomes of *Im3m* inner cubic structures (with Bragg peak positions spaced in the ratio $\cdot 2 : \cdot 4 : \cdot 6$). (B) SAXS patterns of bulk bicontinuous cubic phases of monoolein formed at two different hydration levels (80 wt.% (green plot) and 40 wt.% (red plot) aqueous phase). The sequence of Bragg peak positions spaced in the ratio $\cdot 2 : \cdot 3 : \cdot 4 : \cdot 6 : \cdot 8 : \cdot 9 : \cdot 10 : \cdot 11$ is characteristic of a bicontinuous *Pn3m* double diamond cubic lattice, whereas the sequence of Bragg peak positions spaced in the ratio $\cdot 6 : \cdot 8 : \cdot 14 : \cdot 16 : \cdot 20 : \cdot 22 : \cdot 24 : \cdot 26$ defines a gyroid *Ia3d* cubic lattice structure. Temperature: 20 oC. (C,D) Cryo-TEM images of pep-lipid cubosomes involving the PACAP-DHA double-ligand amphiphile. (C) small cubosome particle of a mixed composition PACAP-DHA/MO/DHA/vitamin E/VPGS-PEG1000 preserving the inner cubic structure of nanochannels upon dispersion from the bulk liquid crystalline phase. (D) A cubosome carrier of PACAP-DHA, for which the Stealth shell is invisible at the nanoparticle periphery due to the insufficient electron density contrast of the PEG chains. The Fast Fourier Transform (FFT) pattern (inset) derived from the cryo-TEM image reveals the *Im3m* inner cubic membrane organization of the pep-lipid cubosome.

The pep-lipid supramolecular assemblies of a cubic phase nanochannel network organization (pep-lipid cubosomes) were obtained at a molar ratio of 1:50 between the DHA-modified peptide amphiphile (PACAP-DHA) and the DHA lipid in the nanocarriers. Under these conditions, we established that the inner cubic structure of the nanoparticulate assemblies (cubosomes) remains stable in the presence of the PACAP-DHA double-ligand amphiphile (Fig. 4A). The sequence of Bragg peak positions spaced in the ratio $\cdot 2 : \cdot 4 : \cdot 6$, and having a first peak at $q=0.104 \text{ \AA}^{-1}$, identified a primitive *Im3m* inner cubic lattice structure of the PEGylated cubosomes. The unit cell dimension was determined to be $a_{Im3m}=14.7 \text{ nm}$ for both the PACAPDHA/MO/DHA/vitamin E/VPGS-PEG1000 and the MO/DHA/vitamin E/VPGS-PEG1000 cubosomes at a lipid molar ratio 69/18/9/4. An additional Bragg peak was observed at $q \cdot 0.11 \text{ \AA}^{-1}$. It was attributed to incompletely PEGylated lipid cubic membrane domains.²² Such domains keep the bicontinuous diamond (*Pn3m*) cubic structure of the non-PEGylated lipid cubic membrane located in the core of the cubosome particles. The cubic unit cell sizes are $a_{Pn3m}=11.1 \text{ nm}$ (orange bar, PACAP-DHA/MO/DHA/vitamin E/VPGS-PEG1000 cubosomes) and $a_{Pn3m}=10.8 \text{ nm}$ (green bar, MO/DHA/vitamin E/VPGS-PEG1000 cubosomes), respectively. Alternatively, a coexisting minor fraction of onion-lamellar-phase particles might explain the peaks observed at $q \cdot 0.11 \text{ \AA}^{-1}$. The latter would correspond to a first-order Bragg reflection of a minor lamellar phase yielding repeat spacings of 5.56 nm (orange bar) or 5.42 nm (green bar).

The SAXS patterns of the bulk MO cubic phases acquired at two hydration levels (80 wt.% and 40 wt.% aqueous phase) are shown in Fig. 4B. The obtained sets of Bragg peaks are characteristic of well ordered liquid crystalline cubic membranous organizations of the nonlamellar lipid matrix. They show that the diminished hydration level leads to a transformation of the bicontinuous double diamond (*Pn3m* crystallographic space group) cubic structure (observed at 80 wt.% aqueous content) into a bicontinuous gyroid (*Ia3d* crystallographic space group) cubic phase (observed at 40 wt.% aqueous content). The cubic unit cell dimensions are dependent on the hydration level ($a_{Pn3m}=10.1 \text{ nm}$ and $a_{Ia3d}=12.8 \text{ nm}$, respectively) in accordance with the MO lipid phase behaviour. Taking into account the experimentally determined unit cell sizes of the bulk lipid cubic phases (Fig. 4B), it is evident that the obtained novel pep-lipid cubosomes comprise swollen-type membrane architectures (Fig. 4A). The encapsulated PACAP-DHA peptide amphiphile did not cause dehydration of the inner nanochannel network structure of the cubosome particles ($a_{Im3m}=14.7 \text{ nm}$).

Topological features of pep-lipid cubosomes

The multicomponent nanoparticulate assemblies PACAP-DHA/MO/DHA/vitamin E/VPGSPEG1000 and MO/DHA/vitamin E/VPGS-PEG1000 (lipid molar ratio 69/18/9/4) were characterized by cryo-TEM imaging. The micrographs presented in Figure 5 demonstrate that the 3D cubic membrane architectures are predominantly present in the mixed pep-lipid assemblies. This finding is in accordance with the obtained SAXS results (Fig. 4A). Under the investigated experimental conditions, the peptide amphiphile PACAP-DHA did not induce the formation of a lamellar layered structure as a predominant phase. As a consequence, the Bragg peak at $q=0.113 \text{ \AA}^{-1}$ can be indexed as a first order reflexion of a minor fraction of a *Pn3m* lipid cubic structure, for which the higher order Bragg peaks remain weak. The latter are visually overlapped by the scattering of the prevailing *Im3m* cubic phase. The inclusion of the peptide amphiphile PACAP-DHA in the self-assembled mixture led to certain morphological changes in the host carrier system (Fig. 5C,D). This structural effect confirmed the encapsulation of PACAP-DHA in the host lipid nanocarriers.

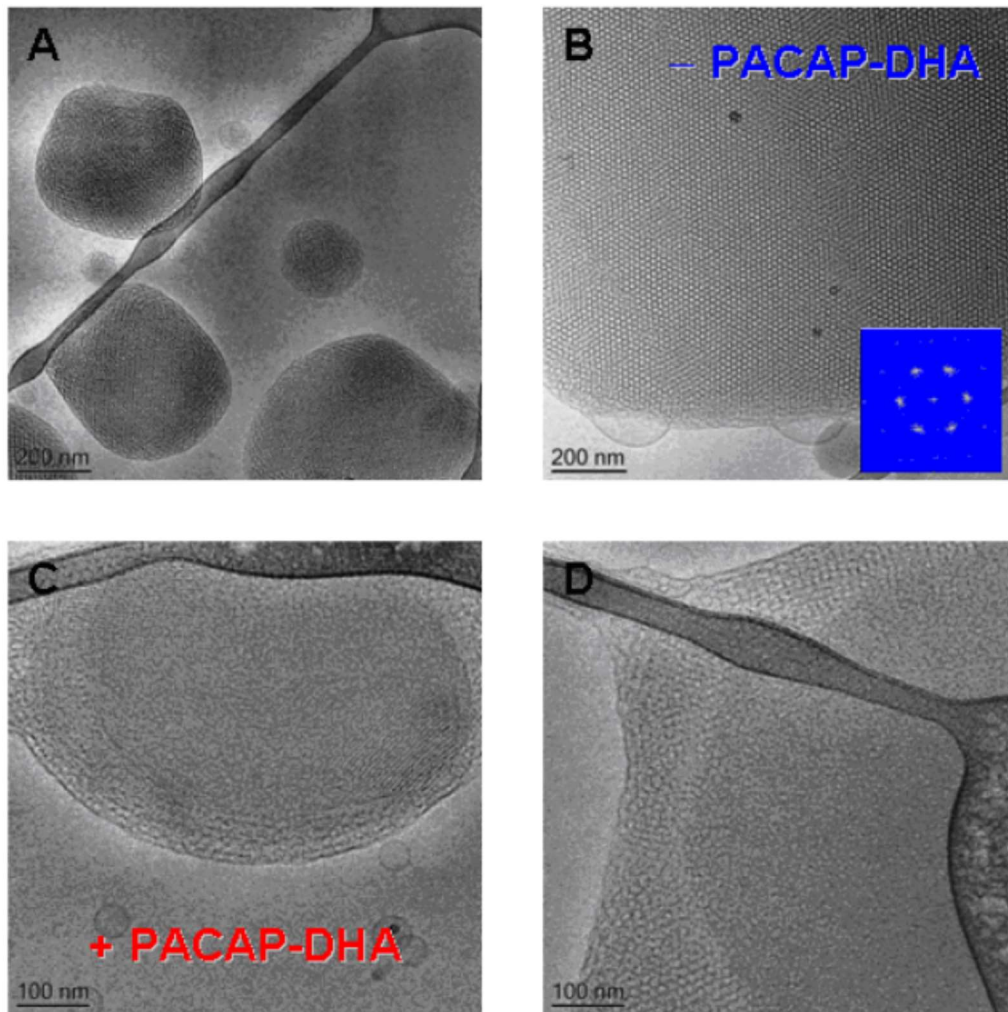


Figure 5. Cryo-TEM images of cubic phase lipid carriers (cubosomes) with multiple functionalities: MO/DHA/vitamin E/VPGS-PEG1000 nanoassemblies (lipid molar ratio 69/18/9/4) before (A,B) and after (C,D) the inclusion of PACAP-DHA. The pep-lipid cubosomes are prepared at a molar ratio 1:50 between PACAP-DHA and DHA. Inset: A Fast Fourier Transform (FFT) pattern derived from the cryo-TEM image in Fig. 5B.

A core-shell organization is apparent for the pep-lipid cubosomes shown in Fig. 5(C,D). The peripheries of the cubosome nanoparticles comprise swollen architectures of nanochannels (Fig. 5D). At variance, the core of the big cubosome particles exhibits a more dense texture of nanochannels (Fig. 5C). The fast Fourier Transform (FFT) pattern of the cryo-TEM image confirmed the cubic lattice periodicity. The resulting hexagonal section corresponds to the projection of the (111) crystallographic plane of the diamond type cubic lattice domain. This organization is generated in cubic domains of large sizes and corresponds to a low degree of PEGylation of the lipid/water interfaces.²²

Figure 4C shows a cryo-TEM image of a small-size pep-lipid cubosome of PACAPDHA/MO/DHA/vitamin E/VPGS-PEG1000 composition, in which the lipid/water interfaces play a more significant role. The perturbation of the cubic lattice liquid crystalline order owing to the insertion of the peptide amphiphile PACAP-DHA in the lipidic cubic lattice network is more essential. The Fast Fourier Transform (FFT) pattern of the image in Fig. 4D evidences a cubic lattice periodicity of the primitive *Im3m* crystallographic space group. The latter corroborates with the SAXS results (Fig. 4A), which deduced a predominant cubic *Im3m* organization of the pep-lipid cubosomes.

The structural features of the pep-lipid cubosomes (PACAP-DHA) can be compared with those established upon building of nanoscale assemblies by other large cationic peptides. For instance, the cationic brain-derived neurotrophic factor (BDNF), characterized by β -sheet

peptide conformation, has been shown to induce the formation of cubic lattice domains and multicompartments organizations in lipid membranous assemblies containing eicosapentaenoic acid (EPA, \sim 3 C20:5).⁷⁹ At variance, the PACAP-DHA peptide amphiphile showed a tendency towards distortion of the long-range liquid crystalline order of the host cubic membrane matrices (Fig. 5). This may be due to partial insertion of the helical peptide moieties in the interfacial lipid headgroup/water regions and altering of the lateral lipid membrane packing in the nanoassemblies.

Despite of the reported variety of nanoparticulate assemblies of liquid crystalline order and hierarchical complexity,^{83–87,91–94} the investigations in which the structural organization of the nanocarriers has been suggested as beneficial for curing of neurodegenerative disease states are scarce.^{6,18,23,36,79} Modifications of GPCR ligands and other neuropeptides by lipophilic anchors can be exploited for enhancement of the peptide drug bioavailability. The proposed here multilevel assembly of bioactive building blocks into nanocarriers represents a step forward the development of disease-modifying drug delivery systems for neurological disorders. The doubleligand PACAP-DHA bioactive conjugate was embedded in biodegradable liquid crystalline nanocarriers, which were stably dispersed as PEGylated particles. The cryo-TEM and SAXS analyses suggested that the new pep-lipid scaffolds of hierarchical organizations can be used in sustained drug-release applications. A slow release modality can be expected thanks to the multicompartments structure of the generated hybrid micello-vesicular containers (Coccinelle patterns). In addition, PEGylation (by varying amounts of the PEGylated amphiphile) may provide increased half-life of the nanoassemblies. All these structural features should contribute to the spatial and temporal regulation of the material transport in the compartmentalized structures, and in particular, of the peptide drug release from the nanocarriers.

The obtained internally nanostructured pep-lipid carriers comprise periodically organized labyrinthine patterns of aqueous nanochannels (cubosomes) (Fig. 5). The realization of channels swelling and gating through alteration of the channels diameter and variation of the nanochannels density is of technological importance for the design of “breathing” soft nanomaterials. Indeed, mesoporous cubic lattice architectures present strong current interest in a number of scientific fields.^{80–94}

The designed here macromolecular building block PACAP-DHA did not show a typical aggregation behaviour of a lipophilic prodrug.³⁰ At variance, unusual pep-lipid containers of compartmentalized structure and high drug content were obtained by spontaneous self-assembly with neuroprotective building blocks. The nanoassembly pathway involves intermediate structures representing the topological transition from mixed micelles to distinct vesicle membrane compartments with ladybird-like (Coccinelle) patterns (Fig. 3). It is remarkable that the observed organized ladybird-like patterns with internal compartments as well as the periodic cubic lipid membrane structures (Fig. 5) mimic the biological compartmentalization in living systems.^{81,82}

The stabilization of the built-up interesting cytoskeleton-like patterns (Fig. 3) may be due to the formation of electrostatic bridges between the charged residues of the peptide amphiphile PACAP-DHA and the carboxylic headgroups of the lipid DHA in the nanocarriers formed at pH 7. Hydrophobic attraction forces between the non-charged regions of the peptide sequences may also contribute to the assembly of neighbouring pep-lipid micelles inside bigger pep-lipid shells. The compact ladybird-like patterns in Figure 3 resemble projections of a network of pep-lipid micelles, which are encapsulated in vesicular membrane shells stabilized by PEG chains. We are not aware of other synthetic pep-lipid assemblies of such sophisticated hierarchical topologies. These soft nanoarchitectures can provide enhanced drug content for therapeutic innovation purposes.

In conclusion, the incorporation of two neurotrophic factors in multicompartments nanocarriers is expected to be advantageous for combination therapy strategies in nanomedicine. Sustained release properties are expected owing to the generated hierarchical multicompartments architectures yielding ladybird-like (Coccinelle) patterns in the cryo-TEM images. Different technological and nanomedicine applications of the PEGylated pep-lipid reservoirs may be envisioned for the nanochannel-type liquid crystalline cubic structures (PACAP-DHA cubosomes) with a capacity for slow release of the amphiphilic drug content.

ASSOCIATED CONTENT

Supporting Information

Supplementary content about the biological roles of DHA and PACAP:

Experimental methods

Figure S1 showing a micellar SAXS pattern.

AUTHOR INFORMATION

Corresponding Authors

*Email: Angelina.Angelova@u-psud.fr ;

*Email: Borislav.Angelov@eli-beams.eu

ORCID

Angelina Angelova: 0000-0002-0285-0637

Markus Drechsler: 0000-0001-7192-7821

Vasil M. Garamus: 0000-0001-9315-4188

Borislav Angelov: 0000-0003-3131-4822

ACKNOWLEDGMENT

The support by the Czech Science Foundation project No.17-00973S and the project Structural dynamics of biomolecular systems (CZ.02.1.01/0.0/0.0/15_003/0000447) from the European Regional Development Fund (ELIBIO) is acknowledged by B.A. The results of the project LQ1606 were obtained with the financial support of the Ministry of Education, Youth and Sports of Czech Republic as a part of the targeted support from the National Program of Sustainability II. M.D. is supported by the collaborative research centre SFB840 of the German Science Foundation DFG. We gratefully acknowledge the allocation of beam time at the Synchrotron Radiation Facility DESY (Deutsche Elektronen Synchrotron, Hamburg, Germany) - storage ring PETRA III, BioSAXS beamline P12 of the European Molecular Biology Laboratory (EMBL) and we thank Dr. C.E. Blanchet for the assistance in using the beamline.

REFERENCES

1. Webber, M.J.; Appel, E.A.; Meijer, E.W.; Langer, R. Supramolecular Biomaterials. *Nat. Mater.* **2016**, *15*, 13–26.
2. Yagmur, A.; Rappolt, M.; Larsen, S.W. In situ Forming Drug Delivery Systems based on Lyotropic Liquid Crystalline Phases: Structural Characterization and Release Properties. *J. Drug Delivery Sci. Tech.* **2013**, *23*, 325–332.
3. Yagmur, A.; Sartori, B.; Rappolt, M.; Self-Assembled Nanostructures of Fully Hydrated Monoelaidin-Elaidic Acid and Monoelaidin-Oleic Acid Systems. *Langmuir* **2012**, *28*, 10105–119.
4. Angelova, A.; Angelov, B.; Mutafchieva, R.; Lesieur, S.; Couvreur, P. Self-Assembled Multicompartment Liquid Crystalline Lipid Carriers for Protein, Peptide, and Nucleic Acid Drug Delivery. *Acc. Chem. Res.*, **2011**, *44*, 147–156.
5. Aleandri, S.; Speziale, C.; Mezzenga, R.; Landau, E.M. Design of Light-Triggered Lyotropic Liquid Crystal Mesophases and their Application as Molecular Switches in 'On demand' release. *Langmuir* **2015**, *31*, 6981–6987.
6. Angelova, A.; Angelov, B.; Drechsler, M.; Lesieur, S. Neurotrophin Delivery using Nanotechnology. *Drug Discovery Today*, **2013**, *18*, 1263–1271.
7. Azhari, H.; Strauss, M.; Hook, S.; Boyd, B.J.; Rizwan, S.B. Stabilising Cubosomes with Tween 80 as a Step towards Targeting Lipid Nanocarriers to the Blood-Brain Barrier. *Eur J Pharm Biopharm* **2016**, *104*, 148–55.
8. G eral, C.; Angelova, A.; Lesieur, S. From Molecular to Nanotechnology Strategies for Delivery of Neurotrophins: Emphasis on Brain-Derived Neurotrophic Factor (BDNF). *Pharmaceutics*, **2013**, *5*, 127–167.
9. van 't Hag, L.; Li, X.; Meikle, T. G.; Hoffmann, S. V.; Jones, N. C.; Pedersen, J. S.; Hawley, A. M.; Gras, S. L.; Conn, C. E.; Drummond, C. J. How Peptide Molecular Structure and Charge Influence the Nanostructure of Lipid Bicontinuous Cubic Mesophases: Model Synthetic WALP Peptides Provide Insights. *Langmuir* **2016**, *32*, 6882–6894.
10. van 't Hag, L.; Shen, H.-H.; Lin, T.-W.; Gras, S. L.; Drummond, C. J.; Conn, C. E. Effect of Lipid-Based Nanostructure on Protein Encapsulation within the Membrane Bilayer Mimetic Lipidic Cubic Phase Using Transmembrane and Lipo-proteins from the Beta-Barrel Assembly Machinery. *Langmuir* **2016**, *32*, 12442–12452.
11. Avinash, M.B.; Govindaraju, T. Nanoarchitectonics of Biomolecular Assemblies for Functional Applications. *Nanoscale*. **2014**, *6*, 13348–69.
12. Gillams, R.J.; Nylander, T.; Plivelic, T.S.; Dymond, M.K.; Attard, G.S. Formation of Inverse Topology Lyotropic Phases in Dioleoylphosphatidylcholine/Oleic Acid and Dioleoylphosphatidylethanolamine/Oleic Acid Binary Mixtures. *Langmuir*, **2014**, *30*, 3337–3344.
13. Black, C.F.; Wilson, R.J.; Nylander, T.; Dymond, M.K.; Attard, G.S. Linear dsDNA Partitions Spontaneously into the Inverse Hexagonal Lyotropic Liquid Crystalline Phases of Phospholipids. *J. Am. Chem. Soc.* **2010**, *132*, 9728–32.
14. Fu, M.; Li, Q.; Sun, B.; Yang, Y.; Dai, L.; Nylander, T.; Li, J. Disassembly of Dipeptide Single Crystals Can Transform the Lipid Membrane into a Network. *ACS Nano* **2017**, *11*, 7349–7354.
15. Rahman, M.M.; Ueda, M.; Hirose, T.; Ito, Y. Spontaneous Formation of Gating Lipid Domain in Uniform-Size Peptide Vesicles for Controlled Release. *J. Am. Chem. Soc.* **2018**, *140*, 17956–17961.
16. Sugihara, K.; Chami, M.; Der enyi, I.; V or os, J.; Zambelli, T. Directed Self-Assembly of Lipid Nanotubes from Inverted Hexagonal Structures. *ACS Nano*, **2012**, *6*, 6626–6632.
17. Bahrami, A.H.; Hummer, G. Formation and Stability of Lipid Membrane Nanotubes. *ACS Nano*. **2017**, *11*, 9558–9565.
18. Guerzoni, L.P.B.; Nicolas, V.; Angelova, A. *In Vitro* Modulation of TrkB Receptor Signaling upon Sequential Delivery of Curcumin-DHA Loaded Carriers Towards Promoting Neuronal Survival. *Pharm. Res.* **2017**, *34*, 492–505.
19. Angelova, A.; Angelov, B.; Garamus, V.M.; Drechsler, M.; A Vesicle-to-Sponge Transition via the Proliferation of Membrane-Linking Pores in ω -3 Polyunsaturated Fatty Acid-Containing Lipid Assemblies. *J. Mol. Liquids* **2019**, *279*, 518–523.
20. Fong, C.; Le, T.; Drummond, C. J. Lyotropic Liquid Crystal Engineering-Ordered Nanostructured Small Molecule Amphiphile Self-assembly Materials by Design. *Chem. Soc. Rev.* **2012**, *41*,

1297-1322.

21. El-Sawy, H.S.; Al-Abd, A.M.; Ahmed, T.A.; El-Say, K.M.; Torchilin, V.P. Stimuli-Responsive Nano-Architecture Drug-Delivery Systems to Solid Tumor Micromilieu: Past, Present, and Future Perspectives. *ACS Nano* **2018**, *12*, 10636-10664.
22. Angelova, A.; Drechsler, M.; Garamus, V.M.; Angelov, B. Liquid Crystalline Nanostructures as Pegylated Reservoirs of Omega-3 Polyunsaturated fatty Acids: Structural Insights toward Delivery Formulations against Neurodegenerative Disorders. *ACS Omega* **2018**, *3*, 3235-3247.
23. Tan, J.; Wang, Y.; Yip, X.; Glynn, F.; Shepherd, R.K.; Caruso, F. Nanoporous Peptide Particles for Encapsulating and Releasing Neurotrophic Factors in an Animal Model of Neurodegeneration *Adv. Mater.* **2012**, *24*, 3362-3366.
24. Angelov, B.; Garamus, V.M.; Drechsler, M.; Angelova, A. Structural Analysis of Nanoparticulate Carriers for Encapsulation of Macromolecular Drugs. *J. Mol. Liquids* **2017**, *235*, 83-89.
25. Kulkarni, J.A.; Darjuan, M.M.; Mercer, J.E.; Chen, S.; van der Meel, R.; Thewalt, J.L.; Tam, Y.Y.C.; Cullis, P.R. On the Formation and Morphology of Lipid Nanoparticles Containing Ionizable Cationic Lipids and siRNA. *ACS Nano*, **2018**, *12*, 4787-4795.
26. Boonruamkaew, P.; Chonpathompikunlert, P.; Vong, L.B.; Sakaue, S.; Tomidokoro, Y.; Ishii, K.; Tamaoka, A.; Nagasaki, Y. Chronic Treatment with a Smart Antioxidative Nanoparticle for Inhibition of Amyloid Plaque Propagation in Tg2576 mouse model of Alzheimer's disease. *Sci Rep.* **2017**, *7*, 3785.
27. Wang, H.X.; Xie, H.Y.; Wang, J.G.; Wu, J.; Ma, X.; Li, L.; Wei, X.; Ling, Q.; Song, P.; Zhou, L.; Xu, X.; Zheng, S. Self-Assembling Prodrugs by Precise Programming of Molecular Structures that Contribute Distinct Stability, Pharmacokinetics, and Antitumor Efficacy. *Adv. Functional Materials* **2015**, *25*, 4956-4965.
28. Zhai, J.; Hinton, T. M.; Waddington, L. J.; Fong, C.; Tran, N.; Mulet, X.; Drummond, C. J.; Muir, B. W. Lipid-PEG Conjugates Sterically Stabilize and Reduce the Toxicity of Phytantriol-Based Lyotropic Liquid Crystalline Nanoparticles. *Langmuir* **2015**, *31*, 10871-10880.
29. Irby, D.; Du, C.; Li, F. Lipid-Drug Conjugate for Enhancing Drug Delivery. *Mol Pharm.* **2017**, *14*, 1325-1338.
30. Gong, X.; Moghaddam, M. J.; Sagnella, S. M.; Conn, C. E.; Danon, S. J.; Waddington, L. J.; Drummond, C. J. Lamellar Crystalline Self-assembly Behaviour and Solid Lipid Nanoparticles of a Palmityl prodrug analogue of Capecitabine—a Chemotherapy Agent. *Colloids Surf. B*, **2011**, *85*, 349-59.
31. Hutchinson, J.A.; Burholt, S.; Hamley, I.W. Peptide Hormones and Lipopeptides: From Self-Assembly to Therapeutic Applications. *J. Peptide Sci.* **2017**, *23*, 82-94.
32. Couvreur, P.; Reddy, L. H.; Mangelot, S.; Poupaert, J. H.; Desmaële, D.; Lepêtre-Mouelhi, S.; Pili, B.; Bourgaux, C.; Amenitsch, H.; Ollivon, M. Discovery of New Hexagonal Supramolecular Nanostructures Formed by Squalenoylation of an Anticancer Nucleoside Analogue. *Small* **2008**, *4*, 247- 253.
33. Lepeltier, E.; Bourgaux, C.; Rosilio, V.; Poupaert, J.H.; Meneau, F.; Zouhiri, F.; Lepêtre-Mouelhi, S.; Desmaële, D.; Couvreur P. Self-Assembly of Squalene-Based Nucleolipids: Relating the Chemical Structure of the Bioconjugates to the Architecture of the Nanoparticles. *Langmuir* **2013**, *29*, 14795-803.
34. Lu, B.; Nagappan, G.; Guan, X.; Nathan, P.J.; Wren, P. BDNF-Based Synaptic Repair as a Disease-Modifying Strategy for Neurodegenerative Diseases. *Nat. Rev. Neurosci.* **2013**, *14*, 401-416.
35. Wong, H.L.; Wu, X.Y.; Bendayan, R. Nanotechnological Advances for the Delivery of CNS Therapeutics. *Adv Drug Deliv Rev.* **2014**, *64*, 686-700.
36. Angelova, A.; Angelov, B. Dual and Multi-Drug Delivery Nanoparticles Towards Neuronal Survival and Synaptic Repair. *Neural Regeneration Research*, **2017**, *12*, 886-889.
37. Pangen, R.; Sharma, S.; Mustafa, G.; Javed, A.; Baboota, S. Vitamin E Loaded Resveratrol Nanoemulsion for Brain Targeting for the Treatment of Parkinson's Disease by Reducing Oxidative Stress. *Nanotechnology* **2014**, *25*, 485102.
38. Sharma, S.; Narang, J.K.; Ali, J.; Baboota, S. Synergistic Antioxidant Action of Vitamin E and Rutin SNEDDS in Ameliorating Oxidative Stress in a Parkinson's Disease Model. *Nanotechnology* **2016**, *27*, 375101.
39. Khanna, S.; Roy, S.; Parinandi, N.L.; Maurer, M.; Sen, C.K. Characterization of the Potent Neuroprotective Properties of the Natural Vitamin E Alpha-Tocotrienol. *J Neurochem.* **2006**, *98*, 1474-1486.
40. Osakada, F.; Hashino, A.; Kume, T.; Katsuki, H.; Kaneko, S.; Akaike, A. Alpha-Tocotrienol Provides the Most Potent Neuroprotection among Vitamin E Analogs on Cultured Striatal Neurons. *Neuropharmacology*. **2004**, *47*, 904-915.
41. Angelova, A.; Garamus, V. M.; Angelov, B.; Tian, Z.; Li, Y.; Zou, A. Advances in Structural Design of Lipid-Based Nanoparticle Carriers for Delivery of Macromolecular Drugs, Phytochemicals and Anti-Tumor Agents. *Adv. Colloid Interface Sci.*, **2017**, *249*, 331-345.
42. Sadeghpour, A.; Sanver, D.; Rappolt, M. Interactions of Flavonoids with Lipidic Mesophases. *Advances in Biomembranes and Lipid Self-Assembly.* **2017**, *25*, 95-123.
43. Bazinet, R.P.; Layé, S. Polyunsaturated Fatty Acids and Their Metabolites in Brain Function and Disease. *Nat Rev Neurosci.* **2014**, *15*, 771-785.
44. Tanaka, K.; Farooqui, A.A.; Siddiqi, N.J.; Alhomid, A.S.; Ong, W.Y. Effects of Docosahexaenoic

- Acid on Neurotransmission. *Biomolec. & Therapeut.* **2012**, *20*, 152–157.
45. Lauritzen, I.; Blondeau, N.; Heurteaux, C.; Widmann, C.; Romey, G.; Lazdunski, M. Polyunsaturated Fatty Acids are Potent Neuroprotectors. *The EMBO J.* **2000**, *19*, 1784–1793.
46. Cutuli, D. Functional and Structural Benefits Induced by Omega-3 Polyunsaturated Fatty Acids During Aging. *Curr Neuropharmacol.* **2017**, *15*, 534–542.
47. Pan, Y.; Khalil, H.; Nicolazzo, J.A. The Impact of Docosahexaenoic Acid on Alzheimer's Disease: Is there a Role of the Blood-Brain Barrier? *Curr. Clin. Pharmacol.* **2015**, *10*, 222–241.
48. Bousquet, M.; Calon, F.; Cicchetti, F. Impact of Omega-3 Fatty Acids in Parkinson's Disease. *Ageing Research Reviews* **2011**, *10*, 453–463.
49. Teng, E.; Taylor, K.; Bilousova, T.; Weiland, D.; Pham, T.; Zuo, X.; Yang, F.; Chen, P.P.; Glabe, C.G.; Takacs, A.; Hoffman, D.R.; Frautschy, S.A.; Cole, G.M. Dietary DHA Supplementation in an APP/PS1 Transgenic Rat Model of AD Reduces Behavioral and A β Pathology and Modulates A β Oligomerization. *Neurobiol. Disease* **2015**, *82*, 552–560.
50. Grimm, M.O.; Kuchenbecker, J.; Grösgen, S.; Burg, V.K.; Hundsdörfer, B.; Rothhaar, T.L.; Friess, P.; de Wilde, M.C.; Broersen, L.M.; Penke, B.; Péter, M.; Vigh, L.; Grimm, H.S.; Hartmann T. Docosahexaenoic Acid Reduces Amyloid β Production via Multiple Pleiotropic Mechanisms. *J. Biol Chem.* **2011**, *286*, 14028–14039.
51. Emendato, A.; Spadaccini, R.; De Santis, A.; Guerrini, R.; D'Errico, G.; Picone, D. Preferential Interaction of the Alzheimer Peptide A β -(1–42) with Omega-3-Containing Lipid Bilayers: Structure and Interaction Studies. *FEBS Lett.* **2016**, *590*, 582–591.
52. de Urquiza, A. M.; Liu, S.; Sjöberg, M.; Zetterström, R. H.; Griffiths, W.; Sjövall, J.; Perlmann, T. Docosahexaenoic Acid, a Ligand for the Retinoid X Receptor in Mouse Brain. *Science* **2000**, *290*, 2140–2144.
53. German, O.L.; Insua, M.F.; Gentili, C.; Rotstein, N.P.; Politi, L.E. Docosahexaenoic Acid Prevents Apoptosis of Retina Photoreceptors by Activating the ERK/MAPK Pathway. *J. Neurochem.* **2006**, *98*, 1507–1520.
54. Levental, K.R.; Lorent, J.H.; Lin, X.; Skinkle, A.D.; Surma, M.A.; Stockenbojer, E.A.; Gorfe, A.A.; Levental, I. Polyunsaturated Lipids Regulate Membrane Domain Stability by Tuning Membrane Order. *Biophysical J.* **2016**, *110*, 1800–10.
55. Eldho, N.V.; Feller, S.E.; Tristram-Nagle, S.; Polozov, I.V.; Gawrisch, K. Polyunsaturated Docosahexaenoic vs Docosapentaenoic Acid-Differences in Lipid Matrix Properties from the Loss of one Double Bond. *J. Am. Chem. Soc.* **2003**, *125*, 6409–6421.
56. Feller, S.E.; Gawrisch, K.; MacKerell, A.D. Jr. Polyunsaturated Fatty Acids in Lipid Bilayers: Intrinsic and Environmental Contributions to their Unique Physical Properties. *J. Am. Chem. Soc.* **2002**, *124*, 318–326.
57. Huster, D.; Arnold, K.; Gawrisch, K. Influence of Docosahexaenoic Acid and Cholesterol on Lateral Lipid Organization in Phospholipid Mixtures. *Biochemistry*, **1998**, *37*, 17299–17308.
58. Shaikh, S.R.; Kinnun, J.J.; Leng, X.; Williams, J.A.; Wassall, S.R. How Polyunsaturated Fatty Acids Modify Molecular Organization in Membranes: Insight from NMR Studies of Model Systems. *Biochim. Biophys. Acta-Biomembranes* **2015**, *1848*, 211–219.
59. Brzustowicz, M.R.; Cherezov, V.; Zerouga, M.; Caffrey, M.; Stillwell, W.; Wassall, S.R. Controlling Membrane Cholesterol Content. A Role for Polyunsaturated (Docosahexaenoate) Phospholipids. *Biochemistry* **2002**, *41*, 12509–12519.
60. Shaikh, S.R.; Cherezov, V.; Caffrey, M.; Stillwell, W.; Wassall, S.R. Interaction of Cholesterol with a Docosahexaenoic Acid-Containing Phosphatidylethanolamine: Trigger for Microdomain/Raft Formation? *Biochemistry* **2003**, *42*, 12028–12037.
61. Guixà-González, R.; Javanainen, M.; Gómez-Soler, M.; Cordobilla, B.; Domingo, J.C.; Sanz, F.; Pastor, M.; Ciruela, F.; Martínez-Seara, H.; Selent, J. Membrane Omega-3 Fatty Acids Modulate the Oligomerisation Kinetics of Adenosine A2A and Dopamine D2 Receptors. *Sci Rep.* **2016**, *6*, 19839.
62. Pinot, M.; Vanni, S.; Pagnotta, S.; Lacas-Gervais, S.; Payet, L.A.; Ferreira, T.; Gautier, R.; Goud, B.; Antonny, B.; Barelli, H. Polyunsaturated Phospholipids Facilitate Membrane Deformation and Fission by Endocytic Proteins. *Science* **2014**, *345*, 693–697.
63. Vanni, S.; Hirose, H.; Barelli, H.; Antonny, B.; Gautier, R. A Sub-Nanometre View of How Membrane Curvature and Composition Modulate Lipid Packing and Protein Recruitment. *Nat Commun.* **2014**, *5*, 4916.
64. Ferrao, R.; Li, J.; Bergamin, E.; Wu, H. Structural Insights in the Assembly of Large Oligomeric Signalosomes in the Toll-Like Receptor/IL-1 Receptor Superfamily. *Sci. Signal.* **2012**, *5*(226), re3.
65. Shaikh, S.R.; Rockett, B.D.; Salameh, M.; Carraway, K. Docosahexaenoic Acid Modifies the Clustering and Size of Lipid Rafts and the Lateral Organization and Surface Expression of MHC class I of EL4 cells. *J. Nutrition* **2009**, *139*, 1632–1639.
66. Angelov, B.; Angelova, A. Nanoscale Clustering of the Neurotrophin Receptor TrkB Revealed by Super-Resolution STED Microscopy. *Nanoscale* **2017**, *9*, 9797–9804.
67. Géral, C.; Angelova, A.; Angelov, B.; Nicolas, N.; Lesieur, S. Chapter 11: Multicompartment Lipid Nanocarriers for Targeting of Cells Expressing Brain Receptors, In "Self-Assembled Supramolecular Architectures: Lyotropic Liquid Crystals". N. Garti, P. Somasundaran, R.

- Mezzenga, Eds. (John Wiley & Sons, Inc., New Jersey, 2012) pp. 319–355.
68. Seaborn, T.; Masmoudi-Kouli, O.; Fournier, A.; Vaudry, H.; Vaudry, D. Protective Effects of Pituitary Adenylate Cyclase-Activating Polypeptide (PACAP) Against Apoptosis. *Curr Pharm Des.* **2011**, *17*, 204–214.
69. Vaudry, D.; Gonzalez, B.J.; Basille, M.; Yon, L.; Fournier, A.; Vaudry, H. Pituitary Adenylate Cyclase-Activating Polypeptide and its Receptors: From Structure to Functions. *Pharmacol Rev.* **2000**, *52*, 269–324.
70. Vaudry, D.; Falluel-Morel, A.; Bourgault, S.; Basille, M.; Burel, D.; Wurtz, O.; Fournier, A.; Chow BK, Hashimoto H, Galas L, Vaudry H. Pituitary Adenylate Cyclase-Activating Polypeptide and Its Receptors: 20 Years after the Discovery. *Pharmacol Rev.* **2009**, *61*, 283–357.
71. R. Yang, X. Jiang, R. Ji, L. Meng, F. Liu, X. Chen, Y. Xin, Therapeutic potential of PACAP for neurodegenerative diseases. *Cell Mol Biol Lett.* **2015**, *20*, 265–278.
72. Reglodi, D.; Kiss, P.; Lubics, A.; Tams, A. Review on the Protective Effects of PACAP in Models of Neurodegenerative Diseases *In Vitro* and *In Vivo*. *Curr Pharm Des.* **2011**, *17*, 962–972.
73. Lee, E.H.; Seo, S. R. Neuroprotective Roles of Pituitary Adenylate Cyclase-Activating Polypeptide in Neurodegenerative Diseases. *BMB Reports* **2014**, *47*, 369–375.
74. Maasz, G.; Zrinyi, Z.; Reglodi, D.; Petrovics, D.; Rivnyak, A.; Kiss, T.; Jungling, A.; Tamas, A.; Pirger, Z. Pituitary Adenylate Cyclase-Activating Polypeptide (PACAP) has a Neuroprotective Function in Dopamine-Based Neurodegeneration in Rat and Snail Parkinsonian Models. *Dis Model Mech.* **2017**, *10*, 127–139.
75. Lazarovici, P.; Cohen, G.; Arien-Zakay, H.; Chen, J.; Zhang, C.; Chopp, M.; Jiang, H. Multimodal Neuroprotection Induced by PACAP38 in Oxygen-Glucose Deprivation and Middle Cerebral artery Occlusion Stroke Models. *J. Mol. Neurosci.* **2012**, *48*, 526–540.
76. Tamas, A.; Reglodi, D.; Farkas, O.; Kovetsdi, E.; Pal, J.; Povlishock, J.T.; Schwarcz, A.; Czeiter, E.; Szanto, Z.; Doczi, T.; Buki, A.; Bukovics, P. Effect of PACAP in Central and Peripheral Nerve Injuries. *Int J Mol Sci.* **2012**, *13*, 8430–8448.
77. Sun, C.; Song, D.; Davis-Taber, R.A.; Barrett, L.W.; Scott, V.E.; Richardson, P.L.; Pereda-Lopez, A.; Uchic, M.E.; Solomon, L.R.; Lake, M.R.; Walter, K.A.; Hajduk, P.J.; Olejniczak, E.T. Solution Structure and Mutational Analysis of Pituitary Adenylate Cyclase-Activating Polypeptide Binding to the Extracellular Domain of PAC1-RS. *Proc Natl Acad Sci U S A.* **2007**, *104*, 7875–7880.
78. Yang, K.; Lei, G.; Jackson, M. F.; MacDonald, J. F. The Involvement of PACAP/VIP System in the Synaptic Transmission in the Hippocampus. *J. Molec Neurosci.* **2010**, *42*, 319–326.
79. Angelov, B.; Angelova, A.; Filippov, S.; Drechsler, M.; Štěpánek, P.; Lesieur, S. Multicompartment Lipid Cubic Nanoparticles with High Protein Upload: Millisecond Dynamics of Formation. *ACS Nano*, **2014**, *8*, 5216–5226.
80. Hyde, S.T. Bicontinuous Structures in Lyotropic Liquid Crystals and Crystalline Hyperbolic Surfaces. *Curr. Opin. Solid State Mater. Sci.* **1996**, *1*, 653–662.
81. Chong, K.; Deng, Y. The Three Dimensionality of Cell Membranes: Lamellar to Cubic Membrane Transition as Investigated by Electron Microscopy. *Methods Cell Biol.* **2012**, *108*, 317–43.
82. Deng, Y.; Almshergii, Z.A. Evolution of Cubic Membranes as Antioxidant Defence System. *Interface Focus* **2015**, *5*, 20150012
83. Kulkarni, C.V.; Yagmur, A.; Steinhart, M.; Kriechbaum, M.; Rappolt, M. Effects of High Pressure on Internally Self-Assembled Lipid Nanoparticles: A Synchrotron Small-Angle X-ray Scattering (SAXS) Study. *Langmuir* **2016**, *32*, 11907–11917.
84. Angelova, A.; Angelov, B.; Garamus, V.M.; Couvreur, P.; Lesieur, S. Small-Angle X-ray Scattering Investigations of Biomolecular Confinement, Loading, and Release from Liquid-Crystalline Nanochannel Assemblies. *J. Phys. Chem. Lett.*, **2012**, *3*, 445–457.
85. Kirkensgaard, J.J.; Evans, M.E.; de Campo, L.; Hyde, S.T. Hierarchical Self-Assembly of a Striped Gyroid Formed by Threaded Chiral Mesoscale Networks. *Proc Natl Acad Sci U S A.* **2014**, *111*, 1271–1276.
86. Angelov, B.; Angelova, A.; Papahadjopoulos-Sternberg, B.; Hoffmann, S.V.; Nicolas, V.; Lesieur, S. Protein-Containing PEGylated Cubosomic Particles: Freeze-Fracture Electron Microscopy and Synchrotron Radiation Circular Dichroism Study. *J. Phys. Chem. B*, **2012**, *116*, 7676–7686.
87. An, T. H.; La, Y.; Cho, A.; Jeong, M. G.; Shin, T. J.; Park, C.; Kim, K. T. Solution Self-Assembly of Block Copolymers Containing a Branched Hydrophilic Block into Inverse Bicontinuous Cubic Mesophases. *ACS Nano* **2015**, *9*, 3084–3096.
88. Angelov, B.; Angelova, A.; Garamus, V.M.; Drechsler, M.; Willumeit, R.; Mutafchieva, R.; Štěpánek, P.; Lesieur, S. Earliest Stage of the Tetrahedral Nanochannel Formation in Cubosome Particles from Unilamellar Nanovesicles. *Langmuir*, **2012**, *28*, 16647–16655.
89. Liu, Q.; Wang, J.; Dong, Y.D.; Boyd, B.J. Using a Selective Cadmium-Binding Peplipid to Create Responsive Liquid Crystalline Nanomaterials. *J. Colloid Interface Sci.* **2015**, *449*, 122–129.
90. Akhlaghi, S.P.; Loh, W. Interactions and Release of Two Palmitoyl Peptides from Phytantriol Cubosomes. *Eur J Pharm Biopharm.* **2017**, *117*, 60–67.
91. Angelova, A.; Ollivon, M.; Campitelli, A.; Bourgaux, C. Lipid Cubic Phases as Stable Nanochannel Network Structures for Protein Biochip Development: X-ray Diffraction Study, *Langmuir*, **2003**, *19*, 6928–6935.
92. Nilsson, C.; Barrios-Lopez, B.; Kallinen, A.; Laurinmäki, P.; Butcher, S. J.; Raki, M.; Weisell, J.;

- Bergström, K.; Larsen, S. W.; Østergaard, J.; Larsen, C.; Urtti, A.; Airaksinen, A. J.; Yaghmur, A. SPECT/CT Imaging of Radiolabeled Cubosomes and Hexosomes for Potential Theranostic Applications. *Biomaterials* **2013**, *34*, 8491-8503.
93. Sun, M.-H.; Huang, S.-Z.; Chen, L.-H.; Li, Y.; Yang, X.-Y.; Yuan, Z.-Y.; Su, B.-L. Applications of Hierarchically Structured Porous Materials from Energy Storage and Conversion, Catalysis, Photocatalysis, Adsorption, Separation, and Sensing to Biomedicine. *Chem. Soc. Rev.* **2016**, *45*, 3479-3563.
94. Höller, R.P.; Dulle, M.; Thomä, S.; Mayer, M.; Steiner, A.M.; Förster, S.; Fery, A.; Kuttner, C.; Chanana, M. Protein-Assisted Assembly of Modular 3D Plasmonic Raspberry-like Core/Satellite Nanoclusters: Correlation of Structure and Optical Properties. *ACS Nano*, **2016**, *10*, 5740-5750.